THE ASTROPHYSICAL JOURNAL, 457:L113–L116, 1996 February 1
© 1996. The American Astronomical Society. All rights reserved. Printed in U.S.A.

ENERGY RELEASE IN A TURBULENT CORONA

G. EINAUDI,[1] M. VELLI,[2] H. POLITANO,[3] AND A. POUQUET[3]
Received 1995 June 26; accepted 1995 October 30

ABSTRACT

Numerical simulations of a two-dimensional section of a coronal loop subject to random magnetic forcing are presented. The forcing models the link between photospheric motions and energy injection in the corona. The results show the highly intermittent spatial distribution of current concentrations generated by the coupling between internal dynamics and external forcing. The total power dissipation is a rapidly varying function of time, with sizable jumps even at low Reynolds numbers, and is caused by the superposition of magnetic dissipation in a number of localized current sheets. Both spatial and temporal intermittency increase with the Reynolds number, suggesting that the turbulent nature of the corona can physically motivate statistical theories of solar activity.

Subject headings: MHD — Sun: flares — turbulence

1. INTRODUCTION

Solar coronal activity is powered by photospheric motions. There is more than enough energy to supply total coronal losses, the main questions being how the energy is deposited and why there are such drastically different signatures of its dissipation (reflected in the large variety of activity manifestations of different energetical importance ranging from heating to large flares). To sustain a large active region, we need a power $W \sim 10^{27}$ ergs s^{-1}. A large flare occurring in the same region gives off $\sim 10^{32}$ ergs on a typical timescale of a few minutes, profoundly affecting the energetics. The measured distribution of flare numbers as a function of energy and duration might be considered as evidence of the highly intermittent nature of coronal magnetohydrodynamic (MHD) turbulence, both in time and in space, which any realistic theory concerning active regions must take into account.

The properties of coronal turbulence, i.e., the way the energy can be stored in the magnetic field and then dissipated, are very difficult to model. In an active region modeled as a cube of side $L = 10^{10}$ cm, the large-scale magnetic Reynolds number for a field of 50 G, density $\sim 10^9$ cm^{-3}, and temperature $\sim 2 \times 10^6$ K is $S \sim 10^{13}$. Assuming a homogeneous and stationary coronal turbulence, the Taylor microscale, defined as the energetically weighted average length over the entire inertial range, is $\lambda \sim S^{-1/2} L \sim 3 \times 10^3$ cm and is independent of the precise power-law spectrum provided the energy decreases with scale (Einaudi & Velli 1994). The dissipative scale, at which the dissipation timescale equals the nonlinear time (i.e., the timescale for the cascade toward small scales to occur), depends on the spectrum, $l \sim S^{-2/3} L \sim 20$ cm, adopting the Kraichnan (1965) description of MHD turbulence. These numbers are indicative and represent orders of magnitude, but there is no doubt that in order to explain solar activity in terms of dissipation of magnetic energy on timescales of seconds or less, the field contributing to the free energy must be structured over spatial scales of the order of 1 m or less, where the local Reynolds number is of order unity. As a result, the local release of magnetic energy occurs on the dynamical timescale and is concentrated inside current sheets which are continuously formed and dissipated throughout the system. Numerical simulations (in two-dimensions) appear to demonstrate that current sheets typically form with a thickness of the order of the dissipative scale l, and width of the order of the Taylor microscale λ (Biskamp & Welter 1989; Diamond & Biskamp 1990). The three-dimensional simulations performed by Mikic, Schnack, & Van Hoven (1989), Strauss (1993), and Longcope & Sudan (1994) show that when a mean large-scale field is assumed in the third direction, it dominates the dynamics in this direction and the perpendicular dynamics is very similar to the two-dimensional case. Such simulations, however, have too low resolution and have been performed for too short times to give reliable information about the long-term response of the corona to the stresses induced by the photospheric motions, whereas the two-dimensional case is obviously less costly.

Here we present some preliminary results of a number of numerical simulations of a two-dimensional section of a coronal loop, subject to random magnetic forcing. The forcing models the link between photospheric motions and energy injection in the corona. Because of the two-dimensional nature of the simulations, it is possible to study the time behavior of the total dissipated power as a function of the dissipative coefficients for times that are long compared to the typical dynamical times of the system and to verify how long it takes for a statistically stationary state to be achieved.

2. A MODEL SIMULATION

Consider a section of a coronal loop threaded by a strong and nowhere vanishing axial magnetic field B_0 whose feet are subject to photospheric random motions. Boundary disturbances propagate along the mean field B_0 with the associated Alfvén velocity and give rise to perpendicular magnetic and velocity fields $b_\perp$ and $v_\perp$. In the limit of a large loop aspect ratio, one may follow the evolution by using the reduced MHD equations (Strauss 1976):

$$\rho\left(\frac{\partial \boldsymbol{v}_\perp}{\partial t} + \boldsymbol{v}_\perp \cdot \boldsymbol{\nabla} \boldsymbol{v}_\perp\right) = -\boldsymbol{\nabla}_\perp\left(p + \frac{1}{2} b_\perp^2\right) + \boldsymbol{b}_\perp \cdot \boldsymbol{\nabla} \boldsymbol{b}_\perp + B_0 \frac{\partial \boldsymbol{b}_\perp}{\partial z} + \boldsymbol{v} \boldsymbol{\nabla}_\perp^2 \boldsymbol{v}_\perp, \quad (1)$$

$$\frac{\partial \boldsymbol{b}_\perp}{\partial t} = \boldsymbol{b}_\perp \cdot \boldsymbol{\nabla} \boldsymbol{v}_\perp - \boldsymbol{v}_\perp \cdot \boldsymbol{\nabla} \boldsymbol{b}_\perp + B_0 \frac{\partial \boldsymbol{v}_\perp}{\partial z} + \eta \boldsymbol{\nabla}_\perp^2 \boldsymbol{b}_\perp. \quad (2)$$

[1] Dipartimento di Fisica, 56100 Pisa, Italy.
[2] Dipartimento di Astronomia e Scienze dello Spazio 50125 Firenze, Italy.
[3] Observatoire de la Côte d'Azur, 06304 Nice Cedex 04, France.

These equations are valid for a plasma with small ratio of kinetic to magnetic pressures, in the limit of a small ratio of poloidal to axial field $b_\perp/B_0 \leq l/L$, where $L/l \gg 1$ is the loop aspect ratio; consequently, the typical velocities are also sub-Alfvénic. The fields $v_\perp$ and $b_\perp$ depend on the axial z-coordinate, though their nonlinear interaction proceeds independently on different constant z surfaces across the loop. Communication across planes is provided by long-wavelength $\lambda \simeq L$ Alfvén waves, which ultimately represent the propagation of energy by photospheric boundary motions. To perform moderate- to high-resolution simulations of the system, we focus on dynamics in a given plane. The terms involving the large-scale axial field thus become unknown random forcing functions, which we must choose in a way consistent with our present understanding of boundary photospheric motions. Thus, we write $B_0(\partial v_\perp/\partial z) = \boldsymbol{F}_m(x, y, t)$, $B_0(\partial \boldsymbol{b}_\perp/\partial z) = \boldsymbol{F}_v(x, y, t)$, where $\boldsymbol{F}_m$ and $\boldsymbol{F}_v$ are our external forcing functions. In the three-dimensional case, on the other hand, one only imposes $v_\perp$ (i.e., $\boldsymbol{F}_m$), on the two photospheric boundary planes. As three-dimensional simulations show that the rms velocity fields remain consistently much smaller than the magnetic fields (i.e., the free energy in the corona is essentially magnetic), we choose to put $\boldsymbol{F}_v = 0$ in our two-dimensional version.

By introducing the vector potential and the stream function, we can transform the two-dimensional MHD equations in two equations for the vector potential and the Laplacian of the stream function (or $-\omega$, where ω is the vorticity). In such equations, the forcing term can be written in the form $\nabla \times f_m \boldsymbol{e}_z = \boldsymbol{F}_m$. The function f_m has a spatial structure which is confined to fairly large scales, so as not to force small-scale dynamics and at the same time to leave some freedom at the larger scales for coherent magnetic structures to emerge via inverse cascade (see, e.g., Politano, Pouquet, & Sulem 1989). In the temporal structure, an "eddy" turnover time t^* appears as follows:

$$f_m = A_1(x, y) \sin^2 (\pi t/2t^*) + A_2(x, y) \sin^2 (\pi t/2t^* + \pi/2),$$

where

$$A_i = \sum_{nm} a^i_{nm} \sin (k_n x + k_m y + \phi^i_{nm}).$$

The k values are chosen in such a way that $3 \leq (k_n^2 + k_m^2)^{1/2} \leq 4$. Every t^*, the a^i_{nm}, and the ϕ^i_{nm} are randomly changed alternately for eddy 1 and eddy 2. The nondimensional spatial rms value of f_m is $\sim$1; this fixes our physical units in terms of the large-scale field B_0 (in velocity units), the typical photospheric velocity $v_{\rm ph}$, the loop length and the aspect ratio. Calling b_0, $l_\perp$, and τ our magnetic field, length, and time units, respectively, we have $1 \sim <f_m> \sim B_0/b_0\ v_{\rm ph}\tau/L$, or

$$b_0 \sim B_0 \left(\frac{l_\perp v_{\rm ph}}{LB_0}\right)^{1/2}, \quad \tau = \frac{l_\perp}{B_0}.$$

For an aspect ratio of 10 and ratio of photospheric velocity to coronal Alfvén speed of about 1/1000, we obtain $b_0/B_0 \simeq 0.01$ and $\tau \simeq 100$ s. We have performed simulations with varying resolutions of 64×64, 128×128, and 256×256 for times from 0 to 550 (i.e., slightly more than 15 hr of real coronal time). The values of resistivity and viscosity are adapted to the grid, so that dissipation coefficients are decreased with increasing resolution. Figure 1 shows the behavior of the spatial average of the current dissipation $\langle \eta J^2 \rangle$ as a function of time for the three different runs. In Table 1 the relevant parameters of each run are summarized along with the corresponding results as average dissipated energy, average magnetic and kinetic energy, and ratio of vorticity to current. In Figure 2 (Plate L6) the vector potential contour lines (above) and the current as a function of position (below) for the high-resolution run at time 496 are shown.

The main results of the simulations can be summarized as follows:

1. The average as well as the maximum dissipation increases with resolution. In passing from a resolution of 64 to 128, there is both a qualitative and a quantitative change in the power dissipation profiles, while in going from 128 to 256 the change is only quantitative: the peaks are similar, though the average at 256 is slightly greater.
2. The ratio of peak to average dissipation also increases with resolution.
3. Input power variations are of the same order of magnitude as the dissipation and occur on the same timescale.
4. The dissipation is concentrated in very localized current sheets separating large-scale magnetic loops (islands in two dimensions).
5. The lifetime of a single current sheet is of the order of the dynamical timescale, and the Reynolds number calculated on the length scale of the current sheets is of the order of 1.
6. The kinetic energy is practically negligible everywhere except in the vicinity of the current sheets, from which quadrupole velocity jets emerge. These jets become locally super-Alfvénic in the higher resolution runs.
7. The global field structure is dominated by an inverse cascade of the vector potential so that, although the forcing contains three to four randomly oriented eddies, the magnetic structures align coherently along any one axis of the numerical domain.
8. Only one timescale appears in the evolution, namely, the dynamical Alfvén time which is faster than our time unit (100 s) by a factor approximately 10, while in the coronal response there is no trace of the forcing time t^*.
9. With increasing resolution, time stationarity is harder to achieve: at resolution of 256, the "flare" at $t \sim 500$ still has a significant impact on the average power dissipated.

3. CONCLUSION

We now discuss the implications of these results on the physics of solar active regions. We have given strong arguments in favor of the fact that the coronal magnetic field subject to smooth, random photospheric flows has the tendency to organize itself in a relatively few large scale tubes separated by narrow current sheets. The idea that photospheric motions induce the formation of current sheets in the corona by displacing the magnetic field line footpoints has been proposed and studied in several ways in the past (Gold 1964; Parker 1972, 1983, 1988, 1991; Sturrock & Uchida 1981; Van Ballegooijen 1986; Mikic et al. 1989; Berger 1991; Chiuderi 1993; Einaudi & Velli 1994; Longcope & Sudan 1994).

We believe that our simulations can contribute toward clarifying a number of points which are unclear or controversial. The ratio of the rms $b_\perp$ produced by photospheric motions to the strong axial field B_0 is much less than 1 and is also smaller than the aspect ratio, so that the approximations leading to our model seem valid. We can evaluate the angle between the rms $b_\perp$ and the axial field by using the data reported in Table 1. It results that the angle increases with

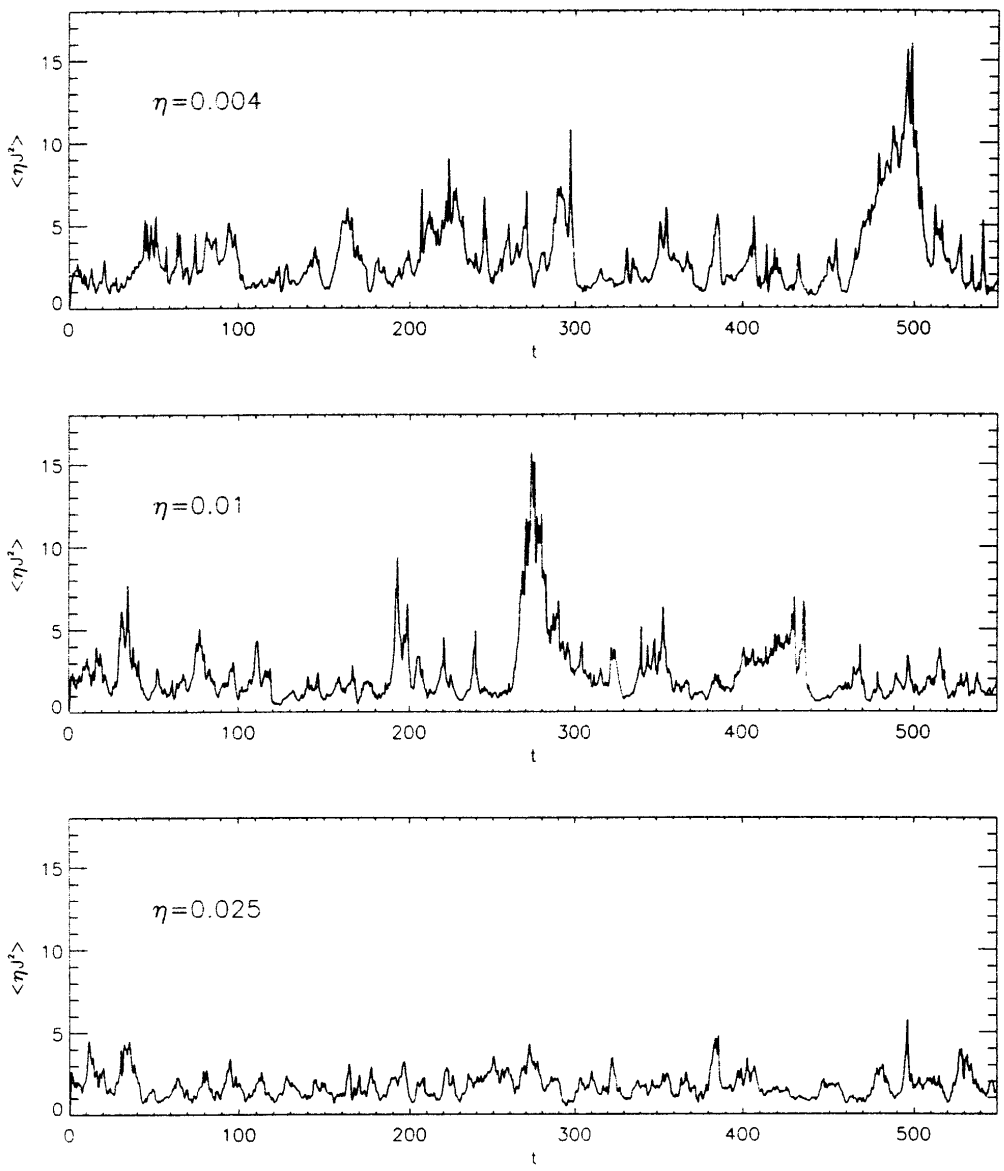

FIG. 1.—Magnetic power dissipation as a function of time for the three runs. *Top*, $n = 256$; *middle*, $n = 128$; *bottom*, $n = 64$.

resolution and is $\theta = 4\overset{\circ}{.}74$ at 256×256, well below the angle hypothesized by Parker.

The fact that the input power produced by the forcing is extremely variable in time is due to the fact that $P_{\rm in} = \boldsymbol{b}_\perp \cdot \boldsymbol{\nabla} \times f_m \boldsymbol{e}_z$. This means that although the forcing varies on a timescale much longer than the coronal dynamical time, the study of the reactions of the corona to photospheric stresses through the stationary MHD ideal equations implies an average over many coronal dynamical times. As a result, all the details are lost; in particular, the rise and disruption of many current sheets are "collapsed" in a single current sheet, the one hypothesized by Parker. The fact that the rms angle defined above is found to be smaller than in the case of Parker is a consequence of the differences between the two models. Here, in contrast to Parker, there is no straightforward relation between the average angle and the dissipation (the rate at which stress develops is an additional dynamical parameter and depends both on the forcing and on the instantaneous field configuration); what really matters in our model is the maximum θ in the region. The maximum value at a given time is reached around the strongest current sheet. For the "flare" occurring at $t = 500$ in the highest resolution simulation, its value is about 20°, while during more quiescent periods it is about 9°. These maximum values are not much greater than those observed at a resolution of 128×128 (which are 20% smaller) and are presumably not far from their "asymptotic" values, since they are quite different from the ones observed at a resolution 64×64: resolution of 64×64 in

TABLE 1

SIMULATION PARAMETERS

Resolution	η, ν	E_m	E_v	P_d	P_v/P_η
64×64	0.025	4.35	1.05	2.65	0.52
128×128	0.01	12.5	1.05	3.16	0.33
256×256	0.004	34.4	0.95	3.54	0.26

the perpendicular plane is not sufficient to describe the features of a high Reynolds number system such as the corona, since the dynamics at that resolution is dominated by resistivity and viscosity, while at 256×256 we begin to be in a more appropriate regime. Hence, all the scalings obtained at lower perpendicular resolution should be taken with some skepticism.

We have tried to investigate a possible link between our results and self-organized criticality or avalanche models. In these models (Lu & Hamilton 1991; Lu et al. 1993; Vlahos et al. 1995). The fundamental ingredient is the non-Gaussianity of the response to a Gaussian forcing which results from the locality of the instability criterion and of the relaxation process. A statistical analysis of the data resulting from our simulations at 256×256 resolution shows evidence of intermittent behavior both in time and space, which means the existence of a non-Gaussian tail in the distribution of the current around its mean (spatial or temporal) value. A detailed discussion of such analysis will be presented in a subsequent paper, because in the present data sets only one "flare" occurs, and therefore we need to integrate our equations for several (real time) days to be able to produce a reliable distribution of event energy release. On the other hand, the time history of the local current sheet can be affected by some explosive phenomenon, such as reconnective instabilities which are known to occur in decaying MHD turbulence, and by waves propagating from other dissipating regions in the system. It is impossible at this stage to define simple rules for this behavior that are amenable to the discrete avalanche models discussed above and to give a physical meaning to an elementary event.

It must also be noted that if, as probable, local electric fields inside current sheets are bigger than the Dreicer field, leading to runaway distribution functions, the MHD approximation fails and the study of the final stage of the build up of the current sheets and their disruption must be performed within the framework of kinetic theory. From a large-scale point of view, the "effective" Reynolds number in the corona due to such kinetic effects could be much smaller than the one derived using classical Spitzer resistivity.

Computations reported in this paper were performed on the Cray of IDRIS (France). This work has received partial financial support from EEC contract ERBCHRXCT930410 and from GdR THEMIS (CNRS).

REFERENCES

Berger, M. A. 1991, A&A, 252, 369
Biskamp, D., & Welter, H. 1989, Phys. Fluids, B1, 1964
Chiuderi, C. 1993, in Scientific Requirements for Future Solar-Physics Space Missions, ed. P. Maltby & B. Battrick (ESA SP-1157), 25
Diamond, P. H., & Biskamp, D. 1990, Phys. Fluids, B2, 681
Einaudi, G., & Velli, M. 1994, in Advances in Solar Physics, ed. G. Belvedere, M. Rodonò, & G. M. Simnett (Berlin: Springer-Verlag), 149
Gold, T. 1964, in The Physics of Solar Flares, ed. W. Hess (NASA SP-50), 389
Kraichnan, R. H. 1965, Phys. Fluids, 8, 1385
Longcope, L., & Sudan, L. 1994, ApJ, 437, 491
Lu, E. T., & Hamilton, R. J. 1991, ApJ, 380, L89
Lu, E. T., Hamilton, R. J., McTiernan, J. M., & Bromund, K. R. 1993, ApJ, 412, 841
Mikic, Z., Schnack, D. D., & Van Hoven, G. 1989, ApJ, 338, 1148
Parker, E. N. 1972, ApJ, 174, 499
———. 1983, ApJ, 264, 642
———. 1988, ApJ, 330, 474
———. 1991, ApJ, 372, 719
Politano, H., Pouquet, A., & Sulem, P. L. 1989, Phys. Fluids, B1, 2330
Strauss, H. 1976, Phys. Fluids, 19, 134
———. 1993, Geophys. Res. Lett., 20, 325
Sturrock, P. A., & Uchida, Y. 1981, ApJ, 246, 331
van Ballegooijen, A. A. 1986, ApJ, 311, 1001
Vlahos, L., Georgoulis, M., Kluiving, R., & Paschos, P. 1995, A&A, 299, 897

PLATE L6

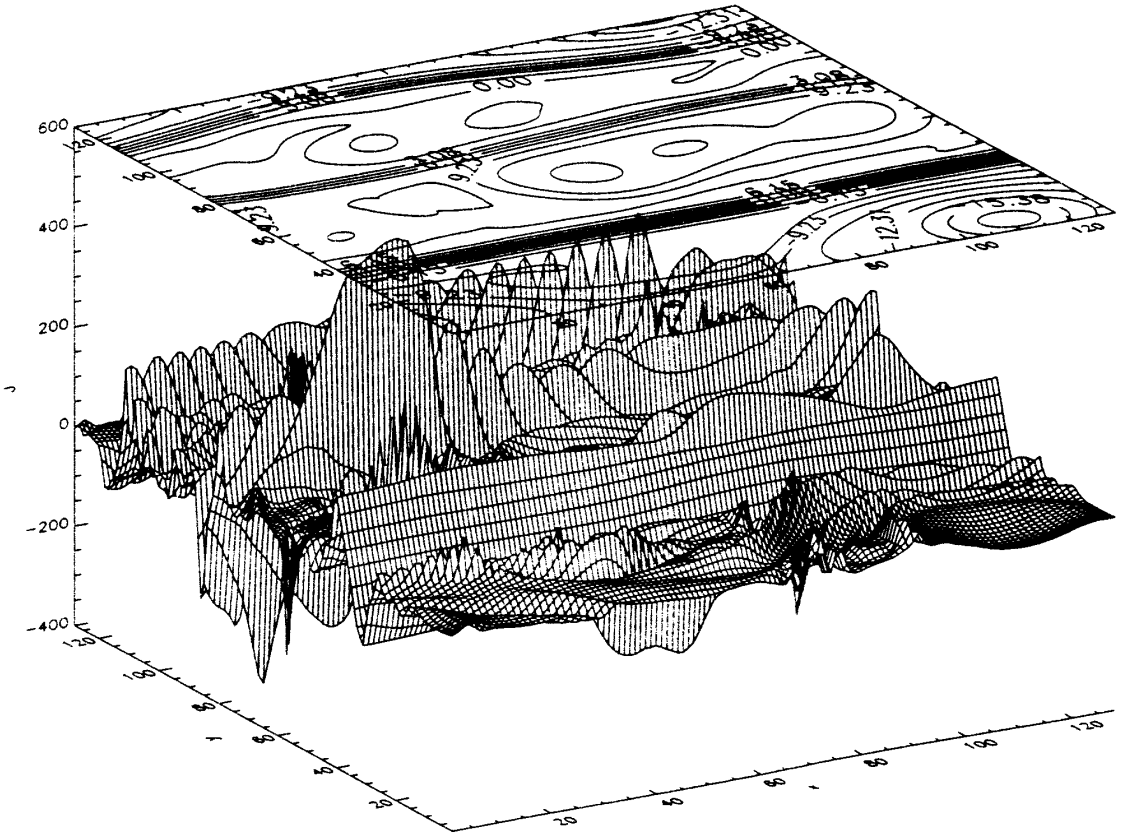

FIG. 2.—Spatial current distribution and vector potential contour lines (i.e., magnetic field lines) for $n = 256$ and time $t = 496$.

EINAUDI et al. (see 457, L114)